Study of waveguide grating eigenmodes for unpolarized filtering applications

Anne-Laure Fehrembach and Anne Sentenac

Institut Fresnel, Centre National de Recherche Scientifique Unité Mixte de Recherche 6133, Faculté de Saint Jérôme (case 162), 13397 Marseille Cedex, France

The dispersion relation of eigenmodes of two-dimensional waveguide gratings is studied with a perturbative model. The analytic expression of the complex wavelength of the modes permits us to predict the shape of the anomalies in the grating reflectivity with respect to the wavelength and the polarization of the incident plane wave. The simultaneous excitation of two independent modes is necessary for obtaining high-efficiency filtering of unpolarized light. We show how this requirement can be met.

OCIS codes: 050.2770, 310.2790, 230.7400, 350.2460.

1. INTRODUCTION

Resonant gratings can be viewed as periodically perturbed planar waveguides. It is well known that the curves of efficiencies of such structures with respect to the wavelength or the angle of incidence may present peaks generated by the excitation of guided waves propagating inside the layers. These anomalies have been widely studied in the case of one-dimensional (1D) gratings illuminated with in-plane mounting, in particular when only one order is reflected and transmitted by the grating.[1] When the periodic perturbation is small, the reflectivity of the structure is close to that of the planar waveguide except when the space and time frequencies imposed by the incident beam are close to those of an eigenmode of the resonant grating. In this case, the reflectivity presents a sharp peak that reaches 100% when the structure has certain symmetry properties.[2] This remarkable behavior, which may be valuable for designing narrowband filters, has motivated a lot of theoretical and experimental work.[3,4] In particular, heuristic models and perturbative approaches have been proposed to determine the influence of the grating parameters (height, filling factor, permittivity, finite length) on the width and centered wavelength of the peak of reflectivity[5,6] and on the angular behavior of the structure.[7] The reflectivity of two-dimensional (2D) resonant gratings and of 1D gratings in conical mounting has been less studied. The first numerical and experimental work concerned 2D square gratings illuminated under normal incidence.[8] These structures are interesting because their filtering properties do not depend on the polarization of the incident beam, in contrast to 1D gratings in classical mounting. Now many technology applications require unpolarized filters working under oblique incidence. This issue has been addressed with 1D lamellar gratings illuminated under off-plane (conical) mounting.[9] Numerical simulations show that a reflectivity peak, irrespective of the incident polarization, is observed for certain values of the filling factor. The same property can be obtained with 2D gratings[10] whose parameters are numerically optimized. A phenomenological theory has recently been presented[11] to explain the reflectivity behavior of 2D resonant gratings as a function of the incident polarization, wavelength, and angle of incidence. It is shown that high-efficiency unpolarized filtering requires the simultaneous excitation of two uncoupled guided waves.

The aim of this paper is to develop a perturbative model that permits us to understand how to obtain the simultaneous excitation of two independent modes with 2D gratings illuminated under oblique incidence. We provide an analytic expression of the complex resonant wavelengths of the modes existing in the waveguide grating for a given real wave vector. Combining this perturbative analysis with the phenomenological theory,[11] we obtain all the features of the filter as a function of the grating parameters.

In Section 2 we sketch the main results of the phenomenological theory. Then we study the eigenmodes of resonant gratings, and we derive their dispersion relation with a perturbative approach. Finally, we illustrate our theory with various numerical simulations.

2. PHENOMENOLOGICAL STUDY OF TWO-DIMENSIONAL RESONANT GRATINGS

A. Presentation of the Structure and Notation

Throughout the paper we use a time dependence in $\exp(-i\omega t)$, and we assume that all media are nonabsorbing. We consider a planar waveguide consisting of a single homogeneous layer with dielectric constant ϵ_l and thickness e along the z axis, embedded in a substrate with dielectric constant ϵ_s, and a superstrate with dielectric constant ϵ_a, with $\epsilon_l > \epsilon_s > \epsilon_a$. For convenience, we introduce the permittivity $\epsilon_{\mathrm{ref}}(z)$ of the planar waveguide, which is equal to ϵ_s, ϵ_l, or ϵ_a depending on whether the abscissa z is located in the substrate, the layer, or the superstrate, respectively. We modify the reference geometry by depositing a grating on top of the layer (Fig. 1). The permittivity $\epsilon(\mathbf{r})$ of the whole structure becomes periodic with periods d_x and d_y along the directions (Ox) and (Oy) in a domain Ω bounded by $z = 0$ and $z = h$. We denote $\epsilon_{\mathrm{per}}(\mathbf{r})$ the periodic permittivity of the perturbation defined as $\epsilon_{\mathrm{per}}(\mathbf{r}) = \epsilon(\mathbf{r}) - \epsilon_{\mathrm{ref}}(z)$, which is equal to 0 outside Ω. The two directions of periodicity are not necessarily orthogonal, as shown in Fig. 2. The recipro-

1084-7529/2003/030481-08$15.00

cal space P of the grating is defined by $P = \{\mathbf{K}_{m,n} = m\mathbf{k}_x + n\mathbf{k}_y,\ (m, n)$ integers$\}$ with $\mathbf{k}_x$ defined by

$$\mathbf{k}_x \cdot \hat{\mathbf{x}} = 2\pi/d_x, \qquad \mathbf{k}_x \cdot \hat{\mathbf{y}} = 0, \tag{1}$$

and similar equations are obtained for $\mathbf{k}_y$ by replacing x with y in Eq. (1).

The resonant grating is illuminated from the superstrate by an incident plane wave characterized by its wave vector $\mathbf{k}_{\mathrm{inc}}$, whose projection onto the Oxy plane is denoted $\mathbf{k}^{\parallel}$, and its wavelength λ_{inc}, [Fig. 1(a)]. To define the polarization of the incident wave, the amplitude of the incident electric field is projected onto two unit vectors,

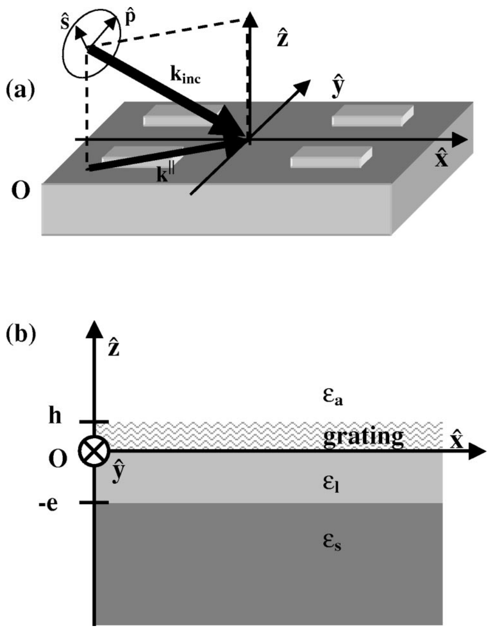

Fig. 1. Notation. (a) Illumination configuration, (b) geometry of the perturbed planar waveguide.

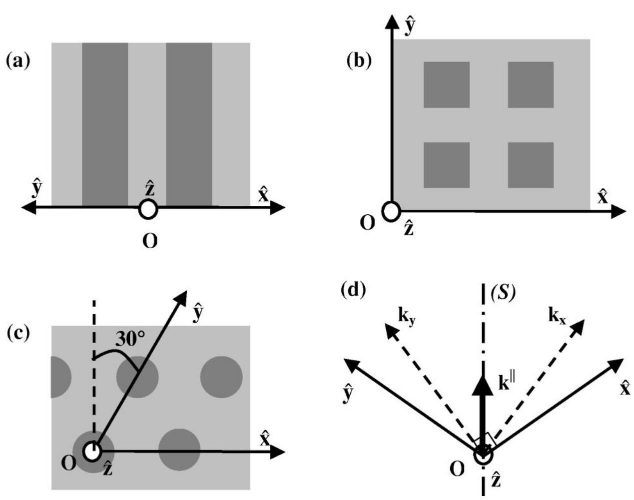

Fig. 2. Top view of the gratings. (a) Lamellar grating periodic along one direction; (b) grating periodic along two orthogonal directions, square bumps; (c) grating periodic along two directions, triangular lattice, circular bumps; (d) Description of the basis in the direct space, $(\hat{\mathbf{x}}, \hat{\mathbf{y}})$, and reciprocal space, $(\mathbf{k}_x, \mathbf{k}_y)$. The bisector of $\hat{\mathbf{x}}$ and $\hat{\mathbf{y}}$ belongs to a vertical plane of symmetry of the structure. The planar incident wave vector $\mathbf{k}^{\parallel}$ is chosen along the bisector of (Ox) and (Oy).

$\hat{\mathbf{s}}_{\mathrm{inc}} = \mathbf{k}_{\mathrm{inc}} \times \hat{\mathbf{z}}/|\mathbf{k}_{\mathrm{inc}} \times \hat{\mathbf{z}}|$ and $\hat{\mathbf{p}}_{\mathrm{inc}}$, where $(\hat{\mathbf{s}}_{\mathrm{inc}}, \mathbf{k}_{\mathrm{inc}}/|\mathbf{k}_{\mathrm{inc}}|, \hat{\mathbf{p}}_{\mathrm{inc}})$ is a direct orthonormal basis. The periods of the grating are assumed to be small enough that only one order is reflected or transmitted. Similarly to the incident field, the transmitted amplitude of the electric field is projected onto two orthonormal s and p vectors belonging to the plane normal to the transmitted direction of propagation. We introduce the 2×2 matrix T that links the s and p projections of the transmitted amplitude to the s and p projections of the incident field. T depends on the spatial and temporal frequencies imposed by the incident beam $(\mathbf{k}^{\parallel}, \lambda_{\mathrm{inc}})$.

B. Reflectivity of Resonant Gratings in the Vicinity of a Resonance

We now assume that the grating's parameters have been chosen in such a way that the structure supports an eigenmode whose pseudoperiodicity is governed by the real spatial frequencies $\mathbf{k}^{\parallel}$ and whose resonant wavelength λ is close to λ_{inc}. The electric field of the mode can be written as

$$\begin{aligned}\mathbf{E}(\mathbf{r}) &= \mathbf{f}(\mathbf{r})\exp(i\mathbf{k}^{\parallel} \cdot \mathbf{r}_{\parallel}) \\ &= \mathbf{f}(\mathbf{r} + md_x\hat{\mathbf{x}} + nd_y\hat{\mathbf{y}})\exp(i\mathbf{k}^{\parallel} \cdot \mathbf{r}_{\parallel}),\end{aligned} \tag{2}$$

with $\mathbf{r} = (\mathbf{r}_{\parallel}, z)$ and (m, n) integers. The resonant wavelength λ is linked to $\mathbf{k}^{\parallel}$ in such a way that the homogeneous equation,

$$\nabla \times \nabla \times \mathbf{E}(\mathbf{r}) - \epsilon(\mathbf{r})\left(\frac{2\pi}{\lambda}\right)^2 \mathbf{E}(\mathbf{r}) = 0, \tag{3}$$

has a nonnull solution in the form of Eq. (2) that satisfies outgoing-wave boundary conditions. In our case, since $\lambda \approx \lambda_{\mathrm{inc}}$ and $|\mathbf{k}^{\parallel}| < \sqrt{\epsilon_a}2\pi/\lambda_{\mathrm{inc}}$, the mode presents propagative outgoing waves in the substrate and superstrate. As a result, the resonant wavelength necessarily has a nonnull imaginary part to account for the leaks.

It is demonstrated[11] that when the incident wavelength is in the vicinity of the real part of the resonant wavelength λ, one and only one eigenvalue of the transmission matrix can be written as

$$l_1^T(\lambda_{\mathrm{inc}}) = u(\lambda_{\mathrm{inc}})\frac{\lambda_{\mathrm{inc}} - \lambda^{T,\mathrm{root}}}{\lambda_{\mathrm{inc}} - \lambda}. \tag{4}$$

Here, both u, $\lambda^{T,\mathrm{root}}$ and λ depend on h. u is a function, with no zeros, close to the eigenvalue of the transmission matrix of the planar waveguide and $\lambda^{T,\mathrm{root}}$ is a complex zero that is introduced for continuity reasons.[11] When the grating height h is diminished, the complex zero $\lambda^{T,\mathrm{root}}$ tends toward λ, whose imaginary part vanishes. In the limit $h = 0$, one retrieves the eigenvalue of the planar waveguide. When the grating is symmetrical with respect to the z axis, $\lambda^{T,\mathrm{root}}$ is real, whatever the periodic perturbation.

The phenomenological theory permits us to analyze with accuracy the behavior of the reflectivity with respect to the incident wavelength. If the polarization vector of the incident beam coincides with the eigenvector $\mathbf{V}_1^T$ of the transmitted matrix T associated with l_1^T, the reflectivity of the structure presents a peak that reaches 100% for symmetrical gratings. The width and position of the peak are given by the imaginary and real parts of λ. In contrast, if the incident polarization vector is orthogonal to $\mathbf{V}_1^T$, the reflectivity remains close to that of the planar waveguide if the periodic perturbation is small. In this case, the incident beam does not couple to the eigenmode. Hence, to get a peak of reflectivity whatever the incident polarization, it is necessary to have two independent eigenmodes with the same wave vector $\mathbf{k}^{\parallel}$ and the same real part of the wavelengths so that both eigenvalues of the T matrix can be written as Eq. (4). This condition is easily fulfilled when $\mathbf{k}^{\parallel} = 0$ and the structure is invariant under a $\pi/2$ rotation.[8] It has proved much more difficult to fulfill when $\mathbf{k}^{\parallel} \neq 0$, i.e., when the filter is used under oblique incidence.

In Section 3 we study the eigenmodes of waveguide gratings and evaluate their complex-resonance wavelength. We show that some structures may support two independent eigenmodes with the same wave vector and the same real part of the wavelength.

3. APPROXIMATE STUDY OF THE EIGENMODES OF A WAVEGUIDE GRATING

Hereafter, we assume that the planar waveguide supports only one guided mode in the domain of spatial and temporal frequencies of the incident beam. We assume that the mode is TE polarized (a similar approach could be derived for TM-polarized modes). We call $\lambda_{\text{ref}}(k)$ the real function that links the resonant wavelength to the modulus of the wave vector of this mode of reference. Since we are interested in a possible mode degeneracy, we choose the grating periods and illumination configuration such that in the limit of $h = 0$, two eigenmodes exist with the same wavevector $\mathbf{k}^{\parallel}$ and the same resonance wavelength close to λ_{inc}. In other words, one can find two different reciprocal space vectors $\mathbf{K}_{p,q}$ and $\mathbf{K}_{u,v}$ such that

$$\lambda_{\text{ref}}(|\mathbf{k}^{\parallel} + \mathbf{K}_{u,v}|) = \lambda_{\text{ref}}(|\mathbf{k}^{\parallel} + \mathbf{K}_{p,q}|) = \lambda^{(0)}. \tag{5}$$

Then we study the change of the resonance wavelengths of these two degenerate modes when the grating height is increased. Throughout the paper, the mode wave vector $\mathbf{k}^{\parallel}$ is kept constant. It is generally observed that the wavelengths of degenerate modes separate when a periodic perturbation is introduced (a local bandgap is opened in the dispersion relation).[1,12] Yet it is possible to reduce the gap between the two wavelengths by minimizing the coupling between the two modes with appropriate grating parameters.[7] In particular, if the grating presents a vertical plane of symmetry (S) and if the wave vector is fixed in this plane of symmetry, the two eigenmodes have different symmetry properties that forbid any coupling between them.[13] It will be shown in the following that is possible to make the gap disappear in this case.

A. Formulation and Resolution of the Homogeneous Equation

It appears convenient for developing our perturbative model to rewrite homogeneous equation (3) satisfied by the eigenmodes in the form

$$\nabla \times \nabla \times \mathbf{E}(\mathbf{r}) - \epsilon_{\text{ref}}(z) k_0^2 \mathbf{E}(\mathbf{r}) = k_0^2 \epsilon_{\text{per}}(\mathbf{r}) \mathbf{E}(\mathbf{r}), \tag{6}$$

with $k_0 = 2\pi/\lambda$. Introducing the Green-tensor solution of

$$\nabla \times \nabla \times \bar{\bar{\mathbf{G}}}(\mathbf{r}_{\parallel} - \mathbf{r}'_{\parallel}, z, z') - \epsilon_{\text{ref}}(z) k_0^2 \bar{\bar{\mathbf{G}}}(\mathbf{r}_{\parallel} - \mathbf{r}'_{\parallel}, z, z') = \delta(\mathbf{r} - \mathbf{r}')\bar{\bar{\mathbf{I}}}, \tag{7}$$

where $\bar{\bar{\mathbf{I}}}$ is the identity tensor, that satisfies an outgoing-wave boundary condition, one transforms differential equation (6) into an integral equation,

$$\mathbf{E}(\mathbf{r}) = k_0^2 \int\int\int_0^h \epsilon_{\text{per}}(\mathbf{r}') \bar{\bar{\mathbf{G}}}(\mathbf{r}_{\parallel} - \mathbf{r}'_{\parallel}, z, z') \mathbf{E}(\mathbf{r}') \mathrm{d}\mathbf{r}'_{\parallel} \mathrm{d}z'. \tag{8}$$

The vector $\mathbf{E}(\mathbf{r})$ is pseudoperiodic, and Eq. (2) can be written as

$$\mathbf{E}(\mathbf{r}) = \sum_m \sum_n \mathbf{E}_{m,n}(z) \exp[i(\mathbf{k}^{\parallel} + \mathbf{K}_{m,n}) \cdot \mathbf{r}_{\parallel}]. \tag{9}$$

The function $\epsilon_{\text{per}}(\mathbf{r})$ is periodic, and we will assume that, for $z \in [0, h]$,

$$\epsilon_{\text{per}}(\mathbf{r}) = \sum_m \sum_n \epsilon_{m,n} \exp(i\mathbf{K}_{m,n} \cdot \mathbf{r}_{\parallel}). \tag{10}$$

The replacement of $\mathbf{E}$ and ϵ_{per} by their Fourier expansions in both members of Eq. (8) finally leads to an infinite set of coupled equations,

$$\mathbf{E}_{m,n}(z) = k_0^2 \sum_j \sum_l \epsilon_{m-j,n-l} \times \int_0^h \bar{\bar{\mathbf{g}}}(\mathbf{K}_{m,n} + \mathbf{k}^{\parallel}, z, z') \mathbf{E}_{j,l}(z') \mathrm{d}z', \tag{11}$$

where $\bar{\bar{\mathbf{g}}}$ is the Fourier transform of $\bar{\bar{\mathbf{G}}}$, defined as

$$\bar{\bar{\mathbf{g}}}(\mathbf{K}_{m,n} + \mathbf{k}^{\parallel}, z, z') = \int\int \bar{\bar{\mathbf{G}}}(\mathbf{r}_{\parallel} - \mathbf{r}'_{\parallel}, z, z') \times \exp(-i(\mathbf{K}_{m,n} + \mathbf{k}^{\parallel}) \cdot (\mathbf{r}_{\parallel} - \mathbf{r}'_{\parallel})) \mathrm{d}\mathbf{r}'_{\parallel}. \tag{12}$$

B. Expansion versus h and Obtaining the Dispersion Relation

In this subsection we consider that the grating height is small compared with the wavelength, and we estimate the complex wavelength λ such that Eq. (11) is satisfied for a nonnull field. We seek λ in the vicinity of $\lambda^{(0)}$ [Eq. (5)]:

$$\lambda - \lambda^{(0)} = O(h). \tag{13}$$

We assume that the electromagnetic field of the mode in the periodically perturbed structure can be written as a power series of h,

$$\mathbf{E}_{m,n}(z) = \mathbf{E}^{(0)}_{m,n}(z) + h\mathbf{E}^{(1)}_{m,n}(z) + O(h^2), \tag{14}$$

where $\mathbf{E}^0_{m,n}(z)$ are the Fourier coefficients of the normalized mode of the planar waveguide at $\lambda = \lambda^{(0)}$. Taking $z = 0$ in Eq. (11) and performing a Taylor development of the integral with respect to h, we obtain the first term of the perturbative expansion,

$$\mathbf{E}_{m,n} = hk_0^2\, \bar{\bar{\mathbf{g}}}_{m,n}(\mathbf{k}^\parallel, \lambda)\sum_j \sum_l \epsilon_{m-j,n-l}\mathbf{E}^{(0)}_{j,l} + O(h^2\, \bar{\bar{\mathbf{g}}}_{m,n}), \tag{15}$$

where

$$\bar{\bar{\mathbf{g}}}_{m,n}(\mathbf{k}^\parallel, \lambda) = \bar{\bar{\mathbf{g}}}(\mathbf{K}_{m,n} + \mathbf{k}^\parallel, 0, 0),\ \ \mathbf{E}_{m,n} = \mathbf{E}_{m,n}(0),$$

and

$$\mathbf{E}^{(0)}_{j,l} = \mathbf{E}^{(0)}_{j,l}(0).$$

1. *Properties of the Green Tensor and of the Mode of the Planar Waveguide*

For convenience, we introduce the set of orthogonal basis $\Gamma_{m,n}$ associated with the direction defined by $\mathbf{K}_{m,n} + \mathbf{k}^\parallel$. The $\Gamma_{m,n}$ basis is defined by the three vectors $(\hat{\mathbf{s}}_{m,n}, \hat{\mathbf{k}}_{m,n}, \hat{\mathbf{z}})$, where $(\hat{\mathbf{k}}_{m,n}) = (\mathbf{K}_{m,n} + \mathbf{k}^\parallel)/|\mathbf{K}_{m,n} + \mathbf{k}^\parallel|$ and $\hat{\mathbf{s}}_{m,n} = \hat{\mathbf{k}}_{m,n} \times \hat{\mathbf{z}}$. In this particular basis, the Fourier transform of the Green tensor is written in the simple form

$$\bar{\bar{\mathbf{g}}}_{m,n}(\mathbf{k}^\parallel, \lambda) = \begin{bmatrix} g^s_{m,n}(\mathbf{k}^\parallel, \lambda) & 0 & 0 \\ 0 & g^k_{m,n}(\mathbf{k}^\parallel, \lambda) & g^{kz}_{m,n}(\mathbf{k}^\parallel, \lambda) \\ 0 & g^{zk}_{m,n}(\mathbf{k}^\parallel, \lambda) & g^z_{m,n}(\mathbf{k}^\parallel, \lambda) \end{bmatrix}. \tag{16}$$

The expressions of the coefficients of $\bar{\bar{g}}_{m,n}$ are given in Appendix A. They involve the reflection coefficients, in both polarizations, of the planar waveguide. These reflection coefficients present poles corresponding to the existence of guided waves in the layer. In our problem, λ is close to the resonant wavelength of a TE guided mode of the unperturbed structure, $\lambda^{(0)}$, which is equal to $\lambda_{\text{ref}}(|\mathbf{k}^\parallel + \mathbf{K}_{p,q}|)$ and $\lambda_{\text{ref}}(|\mathbf{k}^\parallel + \mathbf{K}_{u,v}|)$. Hence $g^s_{p,q}$ and $g^s_{u,v}$ can be cast in the form

$$g^s_{p,q}(\mathbf{k}^\parallel, \lambda) = \frac{A_{p,q}(\mathbf{k}^\parallel, \lambda)}{\lambda - \lambda^{(0)}},\ \ g^s_{u,v}(\mathbf{k}^\parallel, \lambda) = \frac{A_{u,v}(\mathbf{k}^\parallel, \lambda)}{\lambda - \lambda^{(0)}}, \tag{17}$$

where $A_{p,q}$, $A_{u,v}$ are gently varying functions. As a result, $g^s_{p,q}$ and $g^s_{u,v}$ behave as $O(1/h)$ when the wavelength is varied about the resonant wavelength of the reference structure. In contrast, all the other Green coefficients behave as $O(1)$. Moreover, denoting $E^s_{m,n}$, $E^k_{m,n}$, $E^z_{m,n}$ the three components of $\mathbf{E}_{m,n}$ in $\Gamma_{m,n}$, we can see easily that the sole nonnull Fourier coefficients of the mode of the reference structure at $\lambda = \lambda^{(0)}$ are $E^{s(0)}_{p,q}$ and $E^{s(0)}_{u,v}$.

2. *Study of the Real Part of* λ

We project vectorial equations (15) in the $\Gamma_{m,n}$ basis. This is done by introducing the rotation matrices that permit us to change from $\Gamma_{j,l}$ to $\Gamma_{m,n}$. We denote $\psi_{m,n}$ the angle between the vectors $\mathbf{k}^\parallel$ and $\mathbf{K}_{m,n} + \mathbf{k}^\parallel$. Bearing in mind the properties of the Fourier Green tensors and the properties of the mode of the reference structure, we obtain the linear system of equations valid up to first order in h:

$$E^{s(0)}_{p,q} = hk_0^2 g^s_{p,q}(\mathbf{k}^\parallel, \lambda)[\epsilon_{0,0}E^{s(0)}_{p,q} + \epsilon_{p-u,q-v}E^{s(0)}_{u,v} \times \cos(\psi_{p,q} - \psi_{u,v})] + O(h), \tag{18}$$

$$E^{s(0)}_{u,v} = hk_0^2 g^s_{u,v}(\mathbf{k}^\parallel, \lambda)[\epsilon_{0,0}E^{s(0)}_{u,v} + \epsilon_{u-p,v-q}E^{s(0)}_{p,q} \times \cos(\psi_{u,v} - \psi_{p,q})] + O(h). \tag{19}$$

Note that these equations have been derived without any assumption about the shape of the grating. Now we assume that the structure presents a vertical plane of symmetry (S) taken for simplicity along the bisector of the axes (Ox) and (Oy), and we set $\mathbf{k}^\parallel$ in (S); see Fig. 2(d). For each pair of integers (m, n), $\mathbf{K}_{m,n} + \mathbf{k}^\parallel$ is symmetrical with respect to S of $\mathbf{K}_{n,m} + \mathbf{k}^\parallel$ and $\epsilon_{n,m} = \epsilon_{m,n}$. The reciprocal vectors $\mathbf{K}_{p,q}$ and $\mathbf{K}_{u,v}$ are also symmetrical about (S); thus $v = p$ and $u = q$. Moreover, the eigenmodes are either symmetrical or antisymmetrical about (S), which means that $E^s_{m,n} = -\sigma E^s_{n,m}$, $E^k_{m,n} = \sigma E^k_{n,m}$, and $E^z_{m,n} = \sigma E^z_{n,m}$, where $\sigma = 1$ and $\sigma = -1$, respectively. These symmetry properties can be demonstrated by group theory[13] or directly from Eq. (11) by noting that if $\mathbf{E}_{m,n}$ is a solution, then $\mathbf{V}_{m,n}$ with $V^s_{m,n} = E^s_{m,n} \pm E^s_{n,m}$, $V^k_{m,n} = E^k_{m,n} \mp E^k_{n,m}$, $V^z_{m,n} = E^z_{m,n} \mp E^z_{n,m}$ is also a solution. Inserting Eq. (17) into Eq. (18) yields the expression of the wavelengths of the symmetrical and antisymmetrical eigenmodes up to first order in h,

$$\lambda(\mathbf{k}^\parallel) = \lambda^{(0)} + \left(\frac{2\pi}{\lambda^{(0)}}\right)^2 hA_{p,q}(\mathbf{k}^\parallel, \lambda^{(0)}) \times [\epsilon_{0,0} - \sigma\epsilon_{p-q,q-p}\cos(2\psi_{p,q})] + O(h^2). \tag{20}$$

The wavelength λ_{S} of the symmetrical eigenmode is obtained when $\sigma = 1$, and the wavelength λ_{AS} of the antisymmetrical eigenmode is obtained when $\sigma = -1$. Important conclusions can be drawn from the analysis of $(\lambda_{\text{AS}} - \lambda_{\text{S}})$. First, note that the symmetry of the structure and the property of nonabsorption of the materials imply that all the Fourier coefficients of the grating are real. It can also be seen from the expression of the Green tensor given in Appendix A that $\bar{\bar{\mathbf{g}}}_{m,n}(\mathbf{k}^\parallel, \lambda)$ is real as long as $|\mathbf{K}_{m,n} + \mathbf{k}^\parallel| \geqslant \sqrt{\epsilon_s}k_0$. Hence $g^s_{p,q}$ and $A_{p,q}$ are real, and the first term with respect to h of λ_{S} and λ_{AS} is real, too. Hence, when $\epsilon_{p-q,q-p}$ and $\cos(2\psi_{p,q})$ are different from zero and h is small enough, the sign of $(\lambda_{\text{AS}} - \lambda_{\text{S}})$ is given by $\epsilon_{p-q,q-p}\cos(2\psi_{p,q})$. As a consequence, when $\epsilon_{p-q,q-p}$ or $\cos(2\psi_{p,q})$ increases from a negative value to a positive one, $(\lambda_{\text{AS}} - \lambda_{\text{S}})$ inevitably becomes null. This happens for a particular value of $\epsilon_{p-q,q-p}$ or $\cos(2\psi_{p,q})$, which is, in general, slightly different from zero in order to compensate for the contribution of higher orders. Thus it is shown that configurations for which the real parts of λ_{S} and λ_{AS} are strictly the same can be found. This observation explains the results obtained with 1D lamellar resonant gratings illuminated under pure conical mounting (the axis of invariance belongs to the incident plane).[9] By modifying the filling factor, it is possible to superpose the resonance peaks in both p and s polarization. This 1D configuration is a special case of our general study, as will be shown in Section 4. We have verified that the filling factor of the grating that achieves the unpolarized filtering application is optimized such that the Fourier coefficient of the permittivity responsible for the coupling between the modes, $\epsilon_{p-q,q-p}$ is almost null.

3. Study of the Imaginary Part of λ

In order to obtain the imaginary part of λ_S and λ_{AS}, it is necessary to develop Eq. (11) up to second order in h. Considering only the contributions to the imaginary part of the wavelength, the infinite set of coupled linear equations reduces to five equations that is, $E^s_{p,q}$, $E^s_{q,p}$, and the three components of $\mathbf{E}_{0,0}$. Indeed, among all the Fourier Green tensors, only $\bar{\bar{\mathbf{g}}}_{0,0}(\mathbf{k}^{\parallel}, \lambda)$ has a nonnull imaginary part. A rather simple analytical expression for the imaginary part $\mathcal{F}(\lambda)$ of the wavelength is then obtained for both eigenmodes:

$$\begin{aligned}\mathcal{F}[\lambda(\mathbf{k}^{\parallel})] = h^2\left(\frac{2\pi}{\lambda^{(0)}}\right)^4 A_{p,q}(\mathbf{k}^{\parallel}, \lambda^{(0)})|\epsilon_{p,q}|^2 \\ \times [g^s_{0,0}(\mathbf{k}^{\parallel}, \lambda^{(0)})\cos^2(\psi_{p,q})(1-\sigma) \\ + g^k_{0,0}(\mathbf{k}^{\parallel}, \lambda^{(0)}) \\ \times \sin^2(\psi_{p,q})(1+\sigma)] + O(h^3). \qquad (21)\end{aligned}$$

Since $\sigma = 1$ for the symmetrical eigenmode and $\sigma = -1$ for the antisymmetrical one, Eq. (21) expresses that the width of one resonance peak depends on $\cos(\psi_{p,q})$, while the other depends on $\sin(\psi_{p,q})$. Hence the widths of the peaks in the reflectivity curves due to the excitation of a symmetrical or an antisymmetrical mode are different except when $\psi_{p,q}$ is close to 45°. In the configurations proposed by Lacour *et al.*[9] this condition is not satisfied, and the widths of the peaks in p and s polarizations are clearly different. In contrast, in the work of Mizutani *et al.*,[10] unpolarized filters are obtained with hexagonal gratings illuminated along an axis of symmetry in such a way that the angle between the directions of propagation of the two degenerate modes, excited in the limit of $h = 0$, is almost 90°. This implies that $\cos(2\psi_{p,q})$ is close to zero and that $\cos^2(\psi_{p,q})$ is almost equal to $\sin^2(\psi_{p,q})$. In this case, the peaks in s and p polarizations have almost the same width, and they can be easily superposed by slightly varying $\mathbf{k}^{\parallel}$.

4. NUMERICAL EXAMPLES

In this section we present simulations of the dispersion relation and the reflectivity of resonant gratings obtained with a rigorous Fourier modal method.[14] In all examples, $\mathbf{k}^{\parallel}$ is set along the bisector of (Ox), (Oy) that belongs to a vertical plane of symmetry of the structure. The grating periods are chosen such that the incident beam is coupled to a TE eigenmode via the reciprocal space vectors $\mathbf{K}_{1,0}$ and $\mathbf{K}_{0,1}$. Hence the wavelength is varied about $\lambda^{(0)} = \lambda_{\mathrm{ref}}(|\mathbf{k}^{\parallel} + \mathbf{K}_{1,0}|) = \lambda_{\mathrm{ref}}(|\mathbf{k}^{\parallel} + \mathbf{K}_{0,1}|)$.

Our first example is meant to validate the expressions versus h of the resonance wavelengths of the symmetrical and antisymmetrical eigenmodes. We study the dispersion relation of a 1D lamellar grating when $\mathbf{k}^{\parallel}$ is directed along the axis of invariance. This particular configuration can be addressed by our model if we take (Ox) and (Oy) perpendicular to the grating grooves and in opposite directions; see Fig. 2(a), so that $\mathbf{K}_{m,n} = (m-n)2\pi/d\hat{\mathbf{x}}$. In this case, the bisector of (Ox) and (Oy) is the axis of invariance, and it belongs to the vertical plane of symmetry (S) of the structure.

We calculate rigorously the values of the wavelengths $\lambda_S(\mathbf{k}^{\parallel})$ and $\lambda_{AS}(\mathbf{k}^{\parallel})$ of the symmetrical and antisymmetrical modes by seeking the poles of the scattering matrix of the waveguide grating. The latter is evaluated with a Fourier modal method.[14] In Fig. 3 we plot the real part and the square root of the imaginary part of the symmetrical and antisymmetrical wavelengths as a function of h, obtained with the perturbative model (dotted lines) and with the rigorous simulations (solid lines). The planar waveguide has been chosen such that, $\lambda^{(0)} = 1.55\ \mu$m. We verify that the symmetrical and antisymmetrical wavelengths coincide in the limit of $h = 0$ (although the rigorous calculations could not be conducted with enough accuracy for $h < 0.005\ \mu$m). A good agreement between the perturbative and the rigorous results is observed as long as their linear dependence with respect to h is preponderant. When the height is in-

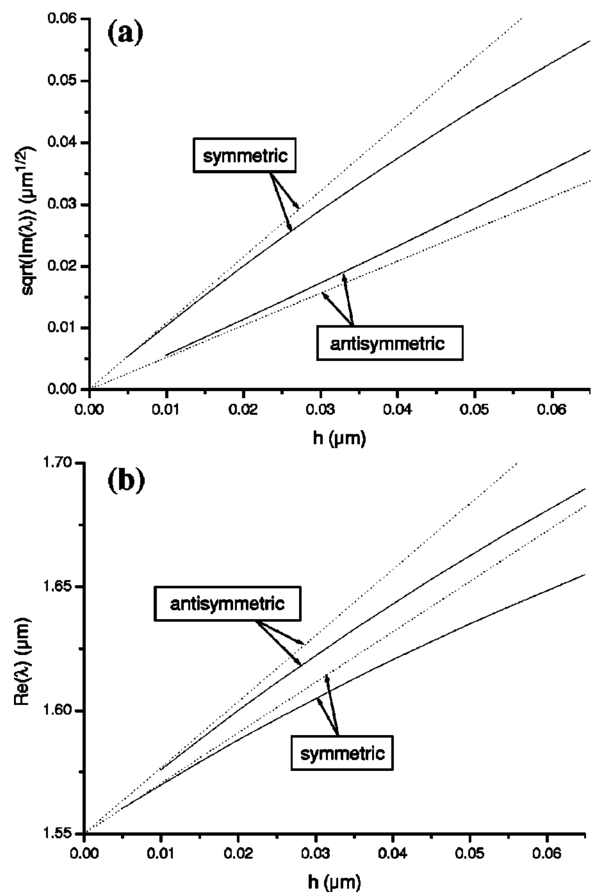

Fig. 3. Comparison of the resonant wavelengths obtained with the rigorous (solid line) and the perturbative (dotted line) methods for both symmetrical and antisymmetrical eigenmodes. The structure is a lamellar grating periodic along one direction with period $d = 864$ nm and filling factor $f = 0.75$, deposited on the planar waveguide described in Fig. 1(b); $e = 130$ nm, $\epsilon_a = 1.0$, $\epsilon_l = 9.0$, $\epsilon_s = 2.25$, $|\mathbf{k}^{\parallel}| = 3.5\ \mu\mathrm{m}^{-1}$. 25 orders (from -12 to $+12$) are used in the Fourier modal method to calculate the resonant wavelength with enough accuracy. (a) Square root of the imaginary part of the resonant wavelengths versus the grating height h, (b) real part of the resonant wavelengths versus h.

creased, the divergence between the two methods is due to the growing influence of the higher orders of the expansion that have not been taken into account. The analytic expressions of the real and imaginary parts of the resonant wavelength, validated by Fig. 3, can be useful in the design of grating filters. Indeed, the real part is related to the centering wavelength of the filter and the imaginary part to its width. In Fig. 3(a) the imaginary part of the symmetrical wavelength is almost four times larger than that of the antisymmetrical one. This implies that the reflectivity peak will be four times wider when the incident beam is p polarized than when it is s polarized. Here we use the fact that the eigenvector $\mathbf{V}_1^T$ of the transmitted matrix associated with a symmetrical mode is directed along $\hat{\mathbf{p}}_{\rm inc}$, whereas that associated with an antisymmetrical mode is directed along $\hat{\mathbf{s}}_{\rm inc}$.[11]

In our second example we show how it is possible to make the real parts of the antisymmetrical and symmetrical wavelengths coincide. We have seen in Section 3 that, all the other parameters being unchanged, the real part of $\lambda_{\rm S} - \lambda_{\rm AS}$ necessarily cancels out for a particular value of $\epsilon_{p-q,q-p}$ ($\epsilon_{-1,1}$ in our case) that is close to but different from zero. This can be done with a 1D lamellar grating illuminated in pure conical mount by taking a filling factor close to (but different from) 0.5.[9] Here we propose an example with a 2D grating periodic along two orthogonal directions (Ox) and (Oy) with the same period d. The pattern is composed of four circular pillars centered on the points $A(d/4, d/4)$, $B(3d/4, d/4)$, $C(d/4, 3d/4)$, $D(3d/4, 3d/4)$; see inset of Fig. 4(a). We change the Fourier coefficients of the grating by modifying the radius $r_{\rm B}$ and $r_{\rm C}$ of the B and C pillars. The vector $\mathbf{k}^{\parallel}$ is set along the bisector of (Ox) and (Oy) that belongs to a vertical plane of symmetry. Again, we search the resonant wavelength $\lambda_{\rm S}$ and $\lambda_{\rm AS}$ in the vicinity of $\lambda_{\rm ref}(|\mathbf{k}^{\parallel} + \mathbf{K}_{1,0}|)$. In Fig. 4(a) we plot the real part of $\lambda_{\rm S} - \lambda_{\rm AS}$ versus $\epsilon_{-1,1}$ obtained with rigorous simulations. As expected from Eq. (20), $\lambda_{\rm S} - \lambda_{\rm AS}$ is quite linear versus $\epsilon_{-1,1}$ when $\epsilon_{-1,1}$ moves away from zero. We note that the real part of $\lambda_{\rm S} - \lambda_{\rm AS}$ cancels out for a particular structure characterized by $\epsilon_{-1,1} = 0.00944$. In Fig. 4(b) we plot the reflectivity of the grating versus the wavelength for both p- and s-polarized incident plane waves. We observe that the peaks are centered about the same wavelength but that their widths differ. This is foreseeable from the expression of the imaginary parts of $\lambda_{\rm S}$ and $\lambda_{\rm AS}$. Indeed, the width of the symmetrical mode peak depends on $\sin(\psi_{1,0})$, whereas the width of the antisymmetrical one depends on $\cos(\psi_{1,0})$. In this simulation, $\psi_{1,0} = 68.46°$.

According to Eqs. (20) and (21), when $\psi_{1,0}$ is close to 45° it is possible to obtain resonance peaks for both polarizations that are centered about the same wavelength and present similar widths. This can be done with a 1D grating, illuminated in pure conical mount,[15] by choosing the period such that $\mathbf{k}_{\parallel} + \mathbf{K}_{1,0}$ is orthogonal to $\mathbf{k}_{\parallel} + \mathbf{K}_{0,1}$. This condition is satisfied when the modulus $k_{\parallel}$ is almost equal to $K_{0,1}$. As a result, the modulus of the wave vector of the reference guided wave $|\mathbf{k}_{\parallel} + \mathbf{K}_{1,0}|$ is close to $\sqrt{2}k_{\parallel}$. Hence the effective index of the mode must necessarily be smaller than $\sqrt{2}$. This requirement is hard to meet in practice since most of the substrates have a refractive index greater than 1.4 in the domain of the wavelengths we are interested in. Less drastic conditions are obtained with 2D gratings. In the following we consider a nonregular triangular lattice with an angle of 80° between the two directions of periodicity (Ox) and (Oy). The angle between the vectors $\mathbf{k}_x$ and $\mathbf{k}_y$ of the reciprocal lattice is 100°; see Fig. 5(a). The pattern is a single circular pillar centered on the point $(d/2; d/2)$, where d is the period along both directions. As usual, the bisecting plane (S) of (Oxz) and (Oyz) is a plane of symmetry. We change $\mathbf{k}^{\parallel}$ in (S) in such a way that $\psi_{1,0}$ varies about 45°. We know that for a given $\psi_{1,0}$ close to 45°, the real part of $\lambda_{\rm AS} - \lambda_{\rm S}$ necessarily cancels out. For this particular incident angle, we plot in Fig. 5(b) the reflectivity curves versus the wavelength for both p and s polarizations. As expected, two peaks centered about the same wavelength and with approximately the same width are observed Hence this structure realizes an unpolarized filter under oblique incidence.

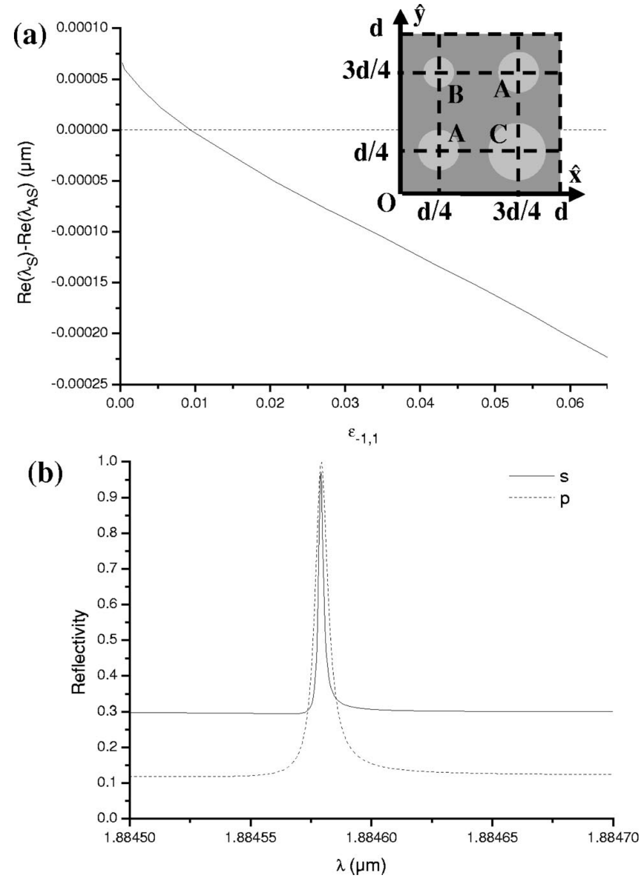

Fig. 4. (a) Difference between the real parts of the symmetrical and the antisymmetrical resonant wavelengths versus the grating Fourier coefficient $\epsilon_{-1,1}$ calculated with the rigorous method. The grating is a square lattice of circular holes of depth $h = 10$ nm, with period $d = 984.3$ nm. $\epsilon_{-1,1}$ is modified by changing the radii of the holes. The holes are drilled in a layer, $\epsilon_l = 4$, $e = 230$ nm, deposited on a substrate, $\epsilon_s = 2.25$, $\epsilon_a = 1$. $|\mathbf{k}^{\parallel}| = 3/\sqrt{2}\ \mu\text{m}^{-1}$. The square cell is discretized into 256 $\times$ 256 square pixels to describe the motif of the grating. $[-3, 3] \times [-3, 3]$ orders along $\mathbf{k}_x$ and $\mathbf{k}_y$ are taken in the Fourier modal method. (b) Reflectivity versus wavelength for p and s incident polarizations of the resonant grating described in (a) when the real part of $\lambda_{\rm AS} - \lambda_{\rm S} = 0$. $\epsilon_{-1,1} = 0.0096$ ($r_A = 123$ nm, $r_B = 38.5$ nm, and $r_C = 196$ nm). The plane of incidence is the bisector of $\hat{\mathbf{x}}$ and $\hat{\mathbf{y}}$, and the angle of incidence with respect to (Oz) is 39.5°.

(a)

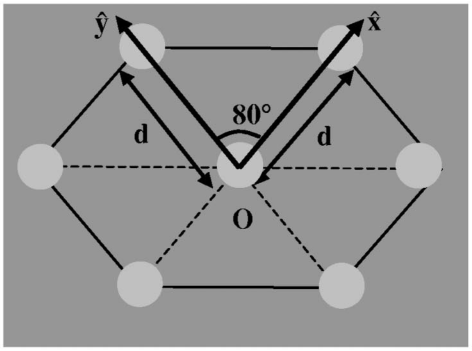

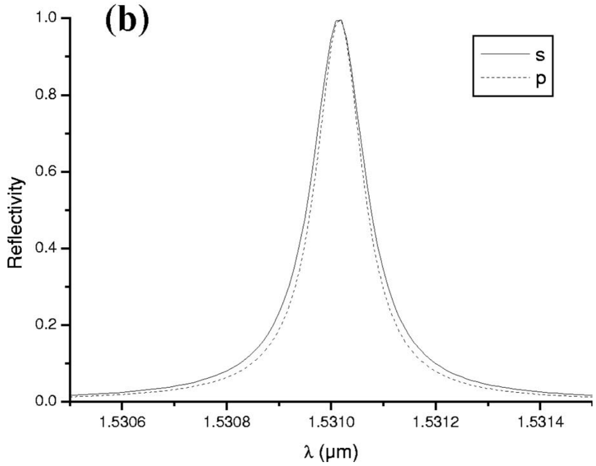

Fig. 5. (a) Top view of the structure whose reflectivity is plotted in (b). The grating is ruled on a multilayer stack that behaves as an antireflection film outside the resonance. The planar waveguide is the superposition of a substrate (dielectric constant 2.097), a first layer (dielectric constant 4.285, thickness 79.1 nm), a second layer (dielectric constant 2.161, thickness 263.5 nm), and a third layer (dielectric constant 4.285, thickness 404.3 nm). The grating consists of circular holes drilled in the third layer (radius 200 nm, depth 30 nm) along a nonregular triangular lattice, with period $d = 953.1$ nm. The diamond-shaped cell is discretized into 256×256 pixels. $[-3, 3] \times [-3, 3]$ orders are taken in the Fourier modal method. (b) Reflectivity of the structure versus wavelength for both s (solid curve) and p (dotted curve) polarizations. The plane of incidence is the bisector of $\hat{\mathbf{x}}$ and $\hat{\mathbf{y}}$, and the angle of incidence is 13.5°.

Note that the condition $\psi_{1,0}$ close to 45° is equivalent to saying that the two modes obtained in the limit $h = 0$ propagate along (almost) orthogonal directions. Geometrical considerations (or the Brewster effect) can then be invoked to explain that in this case, the coupling between the modes that is due to the grating will be very small. However, the frequency gap disappears totally only when the modes have different symmetry properties. Indeed, if the structure is not symmetrical with respect to the plane of incidence (for example, a 1D echelette grating in pure conical mounting), a small frequency gap remains whatever the value of the angle between the directions of propagation of the two guided modes.

5. CONCLUSION

We have presented a perturbative method that gives a simple analytic expression of the complex wavelength of eigenmodes of 2D waveguide gratings existing for a given real wave vector. Combined with a phenomenological theory,[11] this model permits us to predict the reflectivity of resonant gratings illuminated by an incident plane wave as a function of its wavelength and polarization. In order to get a resonance peak irrespective of the polarization, it is necessary to design structures that support two independent eigenmodes for the same wave vector and the same real part of the wavelength. We show that it is possible to obtain such a peak by using gratings that present a vertical plane of symmetry and taking the modes' wave vector in this plane of symmetry. We study the resonance wavelengths of the symmetrical and antisymmetrical eigenmodes and point out that for a certain value of the Fourier coefficient of the permittivity, or for a certain angle of incidence, it is possible to make the real parts of the wavelengths coincide. On the other hand, the imaginary parts remain different in general. Comparisons with rigorous simulations confirm the validity of our approach.

APPENDIX A: FOURIER GREEN TENSORS

In this appendix we write the expressions of $\bar{\bar{\mathbf{g}}}_{m,n}(\mathbf{k}^{\parallel}, \lambda)$ stemming from the analytical formulation of the Fourier transform of the Green tensor[16] $\bar{\bar{\mathbf{g}}}(\mathbf{k}^{\parallel} + \mathbf{K}_{m,n}, z, z')$ with z and z' greater than 0. We obtain

$$g^{s}_{m,n}(\mathbf{k}^{\parallel}, \lambda) = \frac{i\pi}{\gamma^{a}_{m,n}}(1 + R^{s}_{m,n}), \tag{A1}$$

$$g^{k}_{m,n}(\mathbf{k}^{\parallel}, \lambda) = \frac{i\pi\gamma^{a}_{m,n}}{\epsilon_a k_0^2}(1 - R^{p}_{m,n}), \tag{A2}$$

$$g^{kz}_{m,n}(\mathbf{k}^{\parallel}, \lambda) = \frac{i\pi k_{m,n}}{\epsilon_a k_0^2}(-1 - R^{p}_{m,n}), \tag{A3}$$

$$g^{zk}_{m,n}(\mathbf{k}^{\parallel}, \lambda) = \frac{i\pi k_{m,n}}{\epsilon_a k_0^2}(-1 + R^{p}_{m,n}), \tag{A4}$$

$$g^{z}_{m,n}(\mathbf{k}^{\parallel}, \lambda) = \frac{i\pi k^2_{m,n}}{\epsilon_a k_0^2 \gamma^{a}_{m,n}}(1 + R^{p}_{m,n}) - \frac{2\pi}{\epsilon_a k_0^2 h}, \tag{A5}$$

with $R^{s}_{m,n}$ and $R^{p}_{m,n}$ the reflection coefficients of the planar waveguide in s and p polarizations for a tangential wave vector $\mathbf{k}^{\parallel} + \mathbf{K}_{m,n}$ and $k_{m,n} = |\mathbf{k}^{\parallel} + \mathbf{K}_{m,n}|$. The reflection coefficient of the two-layer medium is given by

$$R^{s}_{m,n} = \frac{r_{a,l} + r_{l,s}\exp(i2\gamma^{l}_{m,n}e)}{1 + r_{a,l}r_{l,s}\exp(i2\gamma^{l}_{m,n}e)}, \tag{A6}$$

with

$$r_{\mu,\nu} = \frac{\gamma^{\mu}_{m,n} - \gamma^{\nu}_{m,n}}{\gamma^{\mu}_{m,n} + \gamma^{gn}_{m,n}} \tag{A7}$$

and $\gamma^{\mu}_{m,n} = (\epsilon_\mu k_0^2 - k^2_{m,n})^{0.5}$. The expression for $R^{p}_{m,n}$ is the same as Eq. (A6) with replacement of $\gamma^{\mu}_{m,n}$ by $\gamma^{\mu}_{m,n}/\epsilon_\mu$ and $\gamma^{\nu}_{m,n}$ by $\gamma^{\nu}_{m,n}/\epsilon_\nu$ in the Fresnel reflection coefficients, $r_{\mu,\nu}$.

Anne Sentenac can be reached by e-mail at anne.sentenac@fresnel.fr.

REFERENCES

1. P. Vincent, "Corrugated dielectric waveguides: a numerical study of the second-order stop bands," Appl. Phys. **17**, 239–248 (1978).
2. E. Popov, L. Mashev, and D. Maystre, "Theoretical study of the anomalies of coated dielectric gratings," Opt. Acta **33**, 607–619 (1986).
3. R. Magnusson and S. S. Wang, "New principle for optical filters," Appl. Phys. Lett. **61**, 1022–1024 (1992).
4. A. Sharon, D. Rosenblatt, and A. A. Friesem, "Narrow spectral bandwidths with grating waveguide structures," Appl. Phys. Lett. **69**, 4154–4156 (1996).
5. A. Sharon, D. Rosenblatt, and A. A. Friesem, "Resonant grating-waveguide structures for visible and near-infrared radiation," J. Opt. Soc. Am. A **14**, 2985–2993 (1997).
6. D. Jacob, S. Dunn, and M. G. Moharam, "Design considerations for narrow-band dielectric resonant grating reflection filters of finite length," J. Opt. Soc. Am. A **17**, 1241–1249 (2000).
7. F. Lemarchand, A. Sentenac, E. Cambril, and H. Giovannini, "Study of the resonant behaviour of waveguide gratings: increasing the angular tolerance of guided-mode filters," Pure Appl. Opt. **1**, 545–551 (1999).
8. S. Peng and M. G. Morris, "Resonant scattering from two-dimensional gratings," J. Opt. Soc. Am. A **13**, 993–1005 (1996).
9. D. Lacour, J.-P. Plumey, G. Granet, and A. Mure-Ravaud, "Resonant waveguide grating: analysis of polarization independent filtering," Opt. Quantum Electron. **33**, 451–470 (2001).
10. A. Mizutani, H. Kikuta, K. Nakajima, and K. Iwata, "Nonpolarizing guided-mode resonant grating filter for oblique incidence," J. Opt. Soc. Am. A **18**, 1261–1266 (2001).
11. A.-L. Fehrembach, D. Maystre, and A. Sentenac, "Phenomenological theory of filtering by resonant dielectric gratings," J. Opt. Soc. Am. A **19**, 1136–1144 (2002).
12. N. W. Ashcroft and N. D. Mermin, *Solid State Physics* (Saunders, New York, 1976).
13. K. Sakoda, "Symmetry, degeneracy and uncoupled modes in two-dimensional photonic lattices," Phys. Rev. B **52**, 7982–7986 (1995).
14. L. Li, "New formulation of the Fourier modal method for crossed surface-relief gratings," J. Opt. Soc. Am. A **14**, 2758–2767 (1997).
15. A.-L. Fehrembach, D. Maystre, and A. Sentenac, "Filtering of unpolarized light by gratings," Pure Appl. Opt. **4**, S88–S94 (2002).
16. L. Tsang, J.-A. Kong, and R. T. Shin, *Theory of Microwave Remote Sensing* (Wiley Interscience, New York, 1985).